

A chasmosaurine ceratopsid premaxilla from the basal sandstone of the Hell Creek Formation, Montana

John B. Scannella

Museum of the Rockies, Montana State University, 600 W. Kagy Blvd, Bozeman, Montana, 59717, USA
john.scannella@montana.edu

Abstract: A well-preserved large chasmosaurine ceratopsid premaxilla (MOR 1122 7-22-00-1) collected from the basal sandstone of the Cretaceous Hell Creek Formation (HCF) represents one of the stratigraphically lowest ceratopsid occurrences in the formation. The specimen was discovered in 2000, during the excavation of a large *Torosaurus latus* skull (MOR 1122) which was later hypothesized to represent an advanced growth stage of the more commonly recovered HCF ceratopsid *Triceratops*. MOR 1122 7-22-00-1 compares favorably with the incomplete premaxillae of the MOR 1122 skull and reveals details of premaxilla morphology of ceratopsids from this stratigraphic zone. It preserves large, closely spaced ventromedial foramina, a narrow triangular process, and a thin septal flange at the base of the narial strut. The nasal process is narrow, caudally inclined and has a forked dorsal surface which appears to represent a morphology intermediate between that of the slightly stratigraphically lower ceratopsid *Eotriceratops xerinsularis* from the Horseshoe Canyon Formation of Alberta and specimens recovered higher in the HCF. MOR 1122 7-22-00-1 expresses a deep recess extending medial to the strut of the triangular process, a feature shared with other HCF ceratopsid specimens but not *Eotriceratops* or other earlier occurring triceratopsin taxa. The morphology of MOR 1122 7-22-00-1 is consistent with noted stratigraphic trends in HCF ceratopsids and highlights the increased complexity of the narial region in uppermost Cretaceous triceratopsins.

INTRODUCTION

The uppermost Cretaceous Hell Creek Formation (HCF) of Montana and surrounding regions contains the remains of some of the last non-avian dinosaurs (hereafter referred to as ‘dinosaurs’) to roam western North America (Horner et al. 2011; Clemens and Hartman 2014). An extensive survey of dinosaurs in the HCF near Fort Peck Lake in eastern Montana revealed that approximately 40% of dinosaur skeletons recorded represent the chasmosaurine ceratopsid *Triceratops* (Horner et al. 2011). The abundance of *Triceratops* in the HCF, combined with detailed locality data for most specimens, allows these fossils to be placed within the stratigraphic framework of the formation. Two recognized species (*Triceratops horridus* and *T. prorsus* [Forster 1996]) are stratigraphically separated, with *T. prorsus* being found in the upper unit (U3, sensu Horner et al. 2011) and *T. horridus* is restricted to the lower unit (L3) and the lower part of the middle unit (M3) (Scannella and Fowler 2014; Scannella et al. 2014). Data are consistent

with the presence of an anagenetic lineage of *Triceratops* in which *T. horridus* evolved into *T. prorsus* over the course of the latest Cretaceous (Scannella et al. 2014). Although *Triceratops* is extremely common in the HCF (e.g., Brown 1917; Horner et al. 2011), remains of this animal are less common in the lower unit of the formation (Horner et al. 2011; Scannella and Fowler 2014).

The large HCF *Triceratops* dataset includes members of different ontogenetic stages and reveals a dramatic cranial transformation throughout growth (Goodwin et al. 2006; Horner and Goodwin 2006, 2008). As individuals matured, the postorbital horn cores changed orientation (from caudally to rostrally curved) and the initially triangular epiossifications of the parietal-squamosal frill flattened onto the frill margin (Horner and Goodwin 2006, 2008; Wilson and Fowler 2017). Further morphological and histological evidence indicates that the parietal-squamosal frill of *Triceratops* underwent expansion and eventual fenestration, resulting in a mature morphology previously considered to represent the distinct chasmosaurine *Torosaurus latus*

Published 10 November, 2020

© 2020 by the author; submitted May 8, 2020; revisions received October 24, 2020; accepted October 27, 2020. Handling editor: Robert Holmes. DOI 10.18435/vamp29366

(Scannella and Horner 2010, 2011; Horner and Lamm 2011). This synonymy hypothesis has been the subject of ongoing study and *Torosaurus* is considered a distinct taxon by other authors (see Farke 2011; Longrich and Field 2012; Maiorino et al. 2013). Specimens previously referred to *Torosaurus latus* are relatively rare, being represented by fewer than 20 individuals (e.g., Marsh 1891; Colbert and Bump 1947; Farke 2007; Scannella and Horner 2010; Longrich and Field 2012; Scannella et al. 2014; McDonald et al. 2015) and are more commonly recovered from the lower half of the HCF (Scannella et al. 2014).

In 2000, Merl and Gladys Busenbark discovered Museum of the Rockies (MOR) locality HC-258 ('TORO II') in the basal sandstone of the HCF in Fergus County, Montana, USA (Scannella et al. 2014; Fig. 1). A large, well-preserved partial ceratopsid skull representing one of the most complete examples of '*Torosaurus*' at the time was collected from the site (Farke 2007; Scannella and Horner 2010). Initial excavation was undertaken by Ken Olson and MOR; later excavation was completed by Bob Harmon, Nels Peterson, and the 2000 MOR paleontology field crew. This specimen (MOR 1122; Fig. 2) represents one of the stratigraphically lowest ceratopsid specimens recovered from the HCF of Montana (Scannella et al. 2014). In addition to the MOR 1122 skull, The TORO II quarry also produced the well preserved right premaxilla of a second chasmosaurine ceratopsid (MOR 1122 7-22-00-1, see Figs. 3, 4; Farke 2007). As the premaxillae of MOR 1122 are only partially preserved (Farke 2007), MOR 1122 7-22-00-1 represents

the stratigraphically lowest occurring well-preserved ceratopsid premaxilla from the HCF. Premaxillae are taxonomically informative in chasmosaurine ceratopsids (e.g., Wu et al. 2007; Sampson et al. 2010; Loewen et al. 2010) including *Triceratops*. In *Triceratops prorsus*, the premaxilla contributes to a convex rostrum typically supporting an elongate nasal horn whereas in *Triceratops horridus*, the rostrum is more elongate with the caudally inclined nasal process of the premaxilla (NPP) typically supporting a smaller nasal horn (Forster 1996; Longrich and Field 2012; Scannella et al. 2014, fig. 1; Fig. 5). The base of the HCF has a maximum age of 68 Ma (Fowler 2017). *Eotriceratops xerinsularis*, a slightly earlier occurring triceratopsin (~68.8 Ma, see Wu et al. 2007; Longrich 2011; Eberth and Kamo 2020) from the Horseshoe Canyon Formation of Alberta, is primarily distinguished from *Triceratops* based on the morphology of its premaxilla. Given the rarity of well-preserved ceratopsid premaxillae from the basal sandstone of the HCF, MOR 1122 7-22-00-1 is described here and compared with other latest Maastrichtian specimens.

Institutional abbreviations

AMNH FARB, American Museum of Natural History, Fossil Amphibians, Reptiles, and Birds, New York, USA; MOR, Museum of the Rockies, Bozeman, USA; ROM, Royal Ontario Museum, Toronto, Canada; TMP, Royal Tyrrell Museum of Palaeontology, Drumheller, Canada; UCMP, University of California Museum of Paleontology, Berkeley, USA; YPM, Yale Peabody Museum, New Haven, USA.

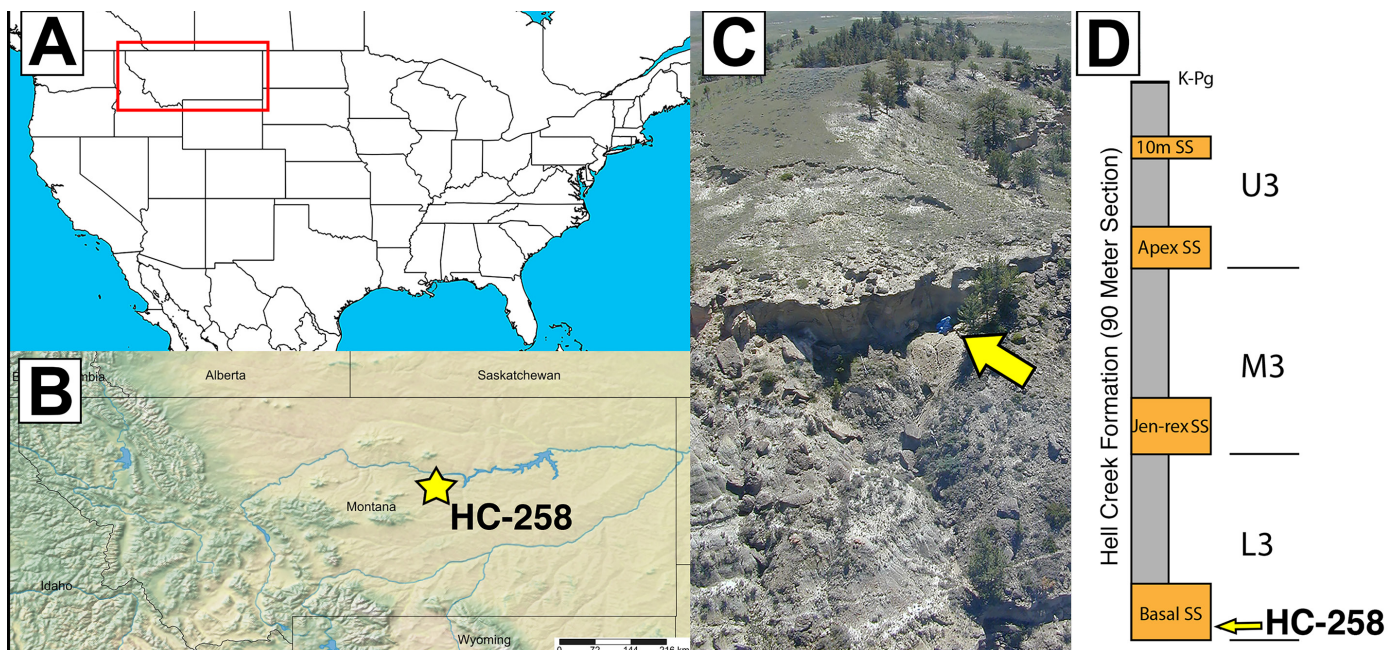


Figure 1. MOR locality HC-258 ('TORO II'). A) Red box highlights Montana and surrounding area. B) HC-258 plotted on a map of Montana. Detailed locality information on file at MOR. A and B created using Simplmappr (simplmappr.net). C) The HC-258 quarry. Image courtesy MOR. D) Stratigraphic position of HC-258 within the Hell Creek Formation. Generalized stratigraphic section of the formation after Horner et al. (2011) and Scannella and Fowler (2014). The bases of the lower (L3), middle (M3), and upper (U3) units are marked by prominent sandstones (Hartman et al., 2014; Scannella and Fowler 2014; Fowler 2016).



Figure 2. Cast of MOR 1122 skull which was found associated with MOR 1122 7-22-00-1. This cast incorporates partial reconstruction of the rostrum (see Farke 2007) and lower jaws of another individual (AMNH FARB 5039). Specimen has a basal skull length of 126.4 cm.

MATERIALS AND METHODS

The specimen MOR 1122 7-22-00-1 was examined at MOR. Measurements were taken using a combination of digital calipers, sliding metal calipers, and a tape measure (measurements over 50 cm). Specimen photos were taken primarily using either a Nikon 1 J2 or Nikon Coolpix B500 camera. Photographs were prepared into figures using Adobe Photoshop and Adobe Illustrator (CC 2018). HCF ceratopsid material at MOR (see Scannella and Fowler, 2014) was examined for direct comparison with MOR 1122 7-22-00-1. Additional material was studied at YPM and the holotype of *Eotriceratops* (TMP 2002.057.007) was examined at TMP.

In order to assess the systematic position of MOR 1122 7-22-00-1, it was added to the specimen level cladistic analysis of HCF ceratopsid specimens conducted in Scannella et al. 2014. The analysis was performed using PAUP* 4.0a (build 168; Swofford 2002) and cladograms were displayed using FigTree (Rambaut 2012). MOR 1122 7-22-00-1 could be coded for 8 of 30 morphological characters (multistate character list from Scannella et al. 2014 presented in Appendix 1, codings presented in Appendix 2). Initially, a branch-and-bound search was performed with MOR 1122 7-22-00-1 added to the Scannella et al. 2014 specimen set which excludes individuals that cannot be coded for at least 10 characters or characters of the frill (18 specimens with *Arrhinoceratops* designated as the outgroup [Scannella et al. 2014, fig. 3B]). Additional analyses were performed using the reduced specimen set (following removal of MOR 2924 from the matrix [Scannella et al. 2014, fig. 3C] and with an alternative coding of the positioning of ventromedial foramina in MOR 981 (see below). An analysis was also performed on the reduced specimen set using only charac-

ters of the premaxilla and excluding specimens which could not be coded for at least three characters.

Geological background

The HCF is divided into three units: the lower third (L3), middle third (M3), and upper third (U3) (Fowler 2009; Horner et al. 2011; Fig. 1). At the base of the formation is an amalgamated channel sandstone termed the basal sandstone, first noted by Brown (1907) and subsequently examined by authors further describing the stratigraphy of the formation (e.g., Flight 2004; Hartman et al. 2014; Fowler 2016, 2017). The base of the HCF has a maximum age of 68 Ma (Fowler 2017). MOR locality HC-258 is positioned within the basal sandstone (Scannella et al. 2014), approximately three meters above the Colgate Member of the underlying Fox Hills Formation (J. Horner, pers. comm. 2019). Dinosaur fossils are relatively rare in the basal sandstone compared to strata higher in the HCF (Horner et al. 2011); however, some exceptionally preserved specimens have been recovered from this sandstone including a partial articulated *Edmontosaurus* (MOR 1142) and a specimen of *Tyrannosaurus rex* which preserves evidence of soft tissues (MOR 1125; Schweitzer et al. 2005; Horner et al. 2011). In addition to remains of the two ceratopsid specimens, the HC-258 quarry also preserved a hadrosaur cervical vertebra (MOR 1122 C-2020-4) and assorted microvertebrate material including a partial theropod phalanx, partial crocodylian osteoderm, piece of trionychid shell, and fragmentary theropod tooth.

DESCRIPTION

MOR 1122 7-22-00-1 (Fig. 3; Tab. 1) is well preserved and nearly complete; it is missing only the caudoventral ‘prong’ and a portion of the medial surface which permits a view of the interior chambers. Some of the thin bone surrounding the septal fossa is missing dorsally, but the rostral margin is preserved. The maximum preserved length is 54.1 cm (Fig. 4; Tab. 1). A pronounced interpremaxillary process divides the ventral margin of the interpremaxillary fenestra into two regions. The caudal region has a maximum width of 7.7 cm and the smaller rostral portion is approximately 5.8 cm wide. This is unlike the condition in the stratigraphically lower *Eotriceratops*, in which the interpremaxillary process appears contiguous with the rostroventral margin of the fenestra, but closely resembles the condition in *Triceratops* found higher in the formation (e.g., MOR 1120, MOR 1625; Fig. 5). Ventral to the interpremaxillary fenestra, several sulci descend from the triangular process towards a shallow depression ventral to the rostral-most portion of the fenestra. The rostral-most portion of this depression exhibits slightly mottled surface texture, similar to that noted on some specimens of

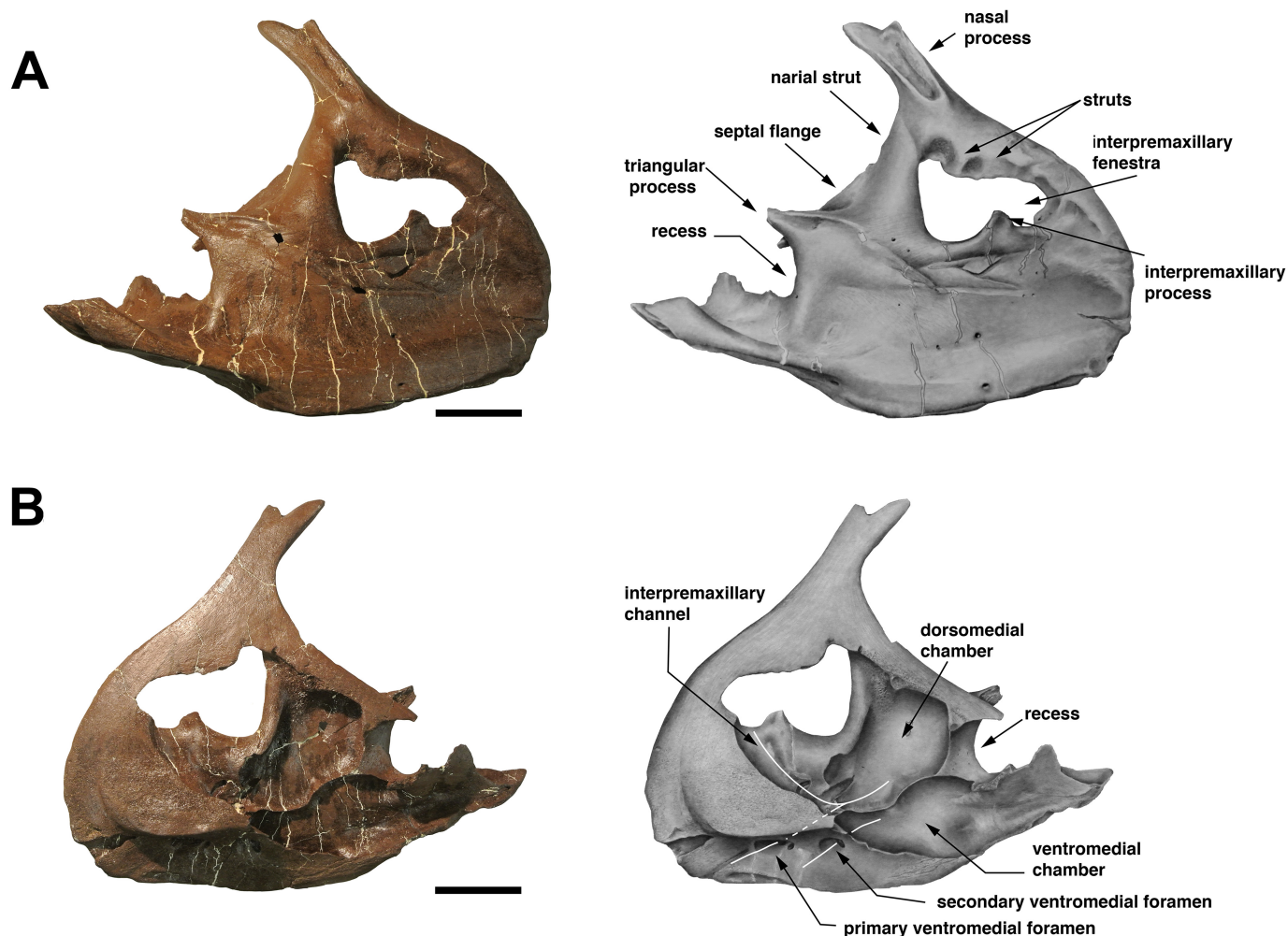


Figure 3. Photographs and illustrations of MOR 1122 7-22-00-1 in A) lateral and B) medial views. White lines indicate hypothesized relationships between ventromedial foramina, interpremaxillary channel, and internal chambers. Scale, 10 cm. Graphite illustrations by K. Scannella.

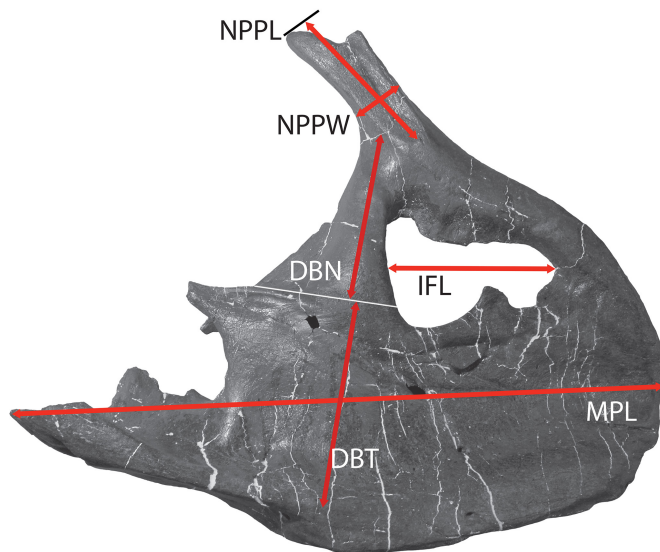
ceratopsid frill (e.g., Brown et al. 2009; Scannella and Horner 2010). A single marked sulcus, which is parallel to those descending from the triangular process, extends from the depression to the rostroventral margin of the premaxilla. Much of the ventral portion of the lateral surface of the premaxilla exhibits a subtle rugose texture with many faint, obliquely oriented striations. Several small foramina are present on the lateral surface of the bone ventral to the interpremaxillary fenestra. A pronounced sulcus located approximately 3 cm ventral to the interpremaxillary process leads to a relatively large foramen (maximum width approximately 1 cm). A similarly sized foramen is positioned approximately 4 cm ventral to the caudal margin of the interpremaxillary fenestra.

The narial strut is relatively broad ventrally and tapers dorsally. Fine striations present on the lateral surface of the strut are oriented roughly parallel to the ventral margin of the premaxilla. A septal flange is present along the caudal margin of the base of the narial strut. The absence of this

septal flange has been used to distinguish *Triceratops* from some other chasmosaurines, including *Pentaceratops* and *Chasmosaurus* (e.g., Forster et al. 1993). However, a septal flange restricted to the base of the narial strut is here noted to be present in some specimens of *Triceratops*, including juveniles (e.g., MOR 1199) and the large subadult YPM 1821 (Fig. 6). Several small foramina are present just lateral to the septal flange. The triangular process (narial process of Wu et al. 2007) bears a prominent dorsocaudally directed strut-like projection which tapers caudally. This process is lateral to the septal flange and exhibits a recess on its lateral surface. The dorsal margin of the triangular process is positioned slightly above the ventral margin of the interpremaxillary fenestra. This is consistent with the position noted in some specimens of *Triceratops* (e.g., AMNH FARB 5116, YPM 1821 [Wu et al. 2007]); the dorsal margin of the triangular process is more distinctly elevated above the ventral margin of the interpremaxillary fenestra in *Eotriceratops* than in *Triceratops* (Wu et al. 2007). A deep

Table 1. Select measurements for MOR 1122 7-22-00-1 (see Figure 4). Measurements in cm.

Maximum preserved length	54.1
NPP Length	14.9
NPP Width	4.9
Dorsoventral breadth of narial strut	15.0
Dorsoventral breadth of triangular process	16.0
Length of interpremaxillary fenestra	15.3
Rostrocaudal diameter of primary foramen	4.0
Rostrocaudal diameter of secondary foramen	2.8

**Figure 4.** Measurement parameters for MOR 1122 7-22-00-1. Measurements presented in Table 1. Abbreviations: NPPL, nasal process of the premaxilla length; NPPW, nasal process of the premaxilla width; IFL, interpremaxillary fenestra length; DBN, dorsoventral breadth of narial strut; DBT, dorsoventral breadth of triangular process; MPL, maximum preserved length.

recess is positioned ventromedial to the strut of the triangular process; this feature is shared with *Triceratops* found higher in the HCF but is not present (or is greatly reduced) in the stratigraphically lower Maastrichtian triceratopsin *Eotriceratops* (Wu et al. 2007). Similarly, this feature is not present in *Regaliceratops peterhewsi* (C. Brown, pers. comm. 2020), which has been recovered within and more recently outside of triceratopsini (Brown and Henderson 2015; Mallon et al. 2016).

The nasal process of the premaxilla (NPP) is elongate, narrow, and caudally inclined, meeting the narial strut at an angle of approximately 124 degrees (Scannella et al. 2014). It bears a shallow facet for articulation with the nasal; the facet exhibits patches of striated and mottled surface textures as well as a series of shallow sulci oriented roughly parallel to the primary trend of the NPP. The dorsal surface of the NPP is forked, bearing a pronounced caudal projection and a smaller rostral projection. These projections are separated by a shallow fossa. In *Eotriceratops*, which slightly predates the HCF (Wu et al. 2007), the NPP is similarly bifurcated although the rostral projection is less pronounced (Fig. 7). In *Eotriceratops*, the NPP is in line with the rostradorsal surface of the premaxilla, whereas in MOR 1122 7-22-00-1 it is deflected slightly dorsally, consistent with the morphology of *T. horridus* (Forster 1996; Scannella et al. 2014). In some HCF ceratopsid specimens (e.g., MOR 1120, MOR 1625), a prominence is noted just rostral to or descending from the narial strut and directed into the interpremaxillary fenestra (Scannella et al. 2014). In MOR 1122 7-22-00-1, there are at least two closely spaced struts directed into the interpremaxillary fenestra, the caudal-most of which originates well rostral to the narial strut, at the rostral-most extent of the facet on the NPP for articulation with the nasal. The caudal-most strut or prominence is similarly placed rostral to the narial strut in YPM 1820, the holotype of *Triceratops horridus* (Fig. 8), and MOR 3011, a specimen from M3 of the HCF (Scannella et al. 2014).

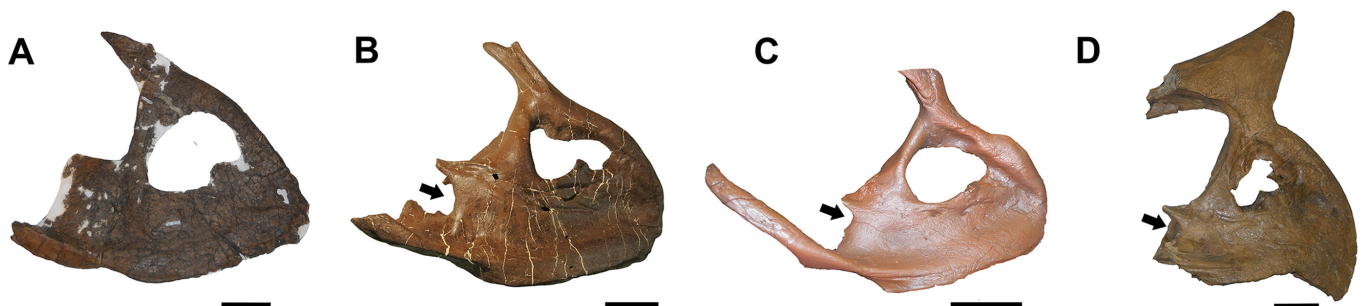
**Figure 5.** Premaxillae in lateral view. A) TMP 2002.057.0007, holotype of *Eotriceratops* (mirrored). B) MOR 1122 7-22-00-1. C) Partially reconstructed cast of MOR 1120, *Triceratops horridus* subadult from L3. D) MOR 1625, *Triceratops prorsus* young adult from U3. The premaxilla of MOR 1625 is fused to the rostral bone, nasal, and epinasal. Arrows highlight the recess positioned ventromedial to the strut of the triangular process. Scale, 10 cm.



Figure 6. Right premaxilla of YPM 1821 (holotype specimen of *Triceratops* ‘*flabellatus*’). Arrow indicates septal flange at the base of the narial strut. Scale, 10 cm. Courtesy of the Division of Vertebrate Paleontology; YPM 1821, Peabody Museum of Natural History, Yale University, New Haven, Connecticut, USA; Peabody.yale.edu.

Much of the internal anatomy of the premaxilla is visible in medial view (Fig. 3B). The medial surface of the NPP is relatively flat and smooth where it would have contacted the opposite premaxilla. A prominent sulcus (here termed the interpremaxillary channel) extends from the rostral portion of the interpremaxillary fenestra towards a series of thin septa which separate the sulcus from dorsomedial and ventromedial premaxillary chambers. The dorsomedial chamber is approximately 15 cm long and the ventromedial chamber extends to the caudal-most preserved extent of the premaxilla. The chambers are separated caudally by a recess located medial to the triangular process (Fig. 3B). The dorsomedial chamber is bound rostr dorsally by a ridge caudoventral to the interpremaxillary fenestra. Two smaller (approximately 1 cm wide), shallow sulci extend from the ventral surface onto the lateral surface of the interpremaxillary channel. The caudal-most sulcus connects the interpremaxillary channel to the dorsomedial chamber and leads to

the largest foramen noted on the lateral surface, ventral to the interpremaxillary fenestra. The two largest ventromedial foramina (here termed the primary and secondary foramen) are contiguous with the premaxillary chambers (Fig. 3B). The larger primary foramen (approximately 4 cm wide) leads into the interpremaxillary channel which connects to the dorsomedial chamber; the smaller secondary foramen (approximately 2.8 cm wide) leads directly into the ventromedial chamber. These foramina are closely spaced (2.9 cm distance between the caudal margin of primary foramen and rostral margin of the secondary foramen). Although the right premaxilla of the articulated MOR 1122 skull is incomplete, the morphology of the ventromedial foramina compares favorably with MOR 1122 7-22-00-1 (Figs. 9, 10B, C). In MOR 1122, these foramina are 3.4 cm apart. The primary ventromedial foramen is partially bordered rostrally by an obliquely oriented margin (Fig. 9). Though incomplete, it indicates a minimum diameter of 2.4 cm for the primary ventromedial foramen. The ventromedial foramina of MOR 3081, a ‘*Torosaurus*’ specimen from the upper part of the lower HCF, are also relatively large and closely spaced (Fig. 10D). The stratigraphically lower *Eotriceratops* also exhibits closely spaced ventromedial foramina (Fig. 10A; Scannella et al. 2014). *Triceratops* recovered from higher in the HCF typically exhibit more widely spaced ventromedial foramina (Figs. 10E–G, 11; Table 2); though in some specimens of *Triceratops* the foramina may be more closely spaced (Hatcher et al. 1907, fig. 28). A small additional foramen is located in the caudolateral margin of the primary foramen of MOR 1122-7-22-00-1; a shallow sulcus extends rostroventrally from this foramen. Approximately 3.8 cm rostral to the primary foramen, an additional foramen is present and extends into a relatively wide (approximately 2 cm) sulcus rostroventrally. Ventrally, a groove for articulation with the rostral bone extends lateral to the ventromedial foramina for approximately

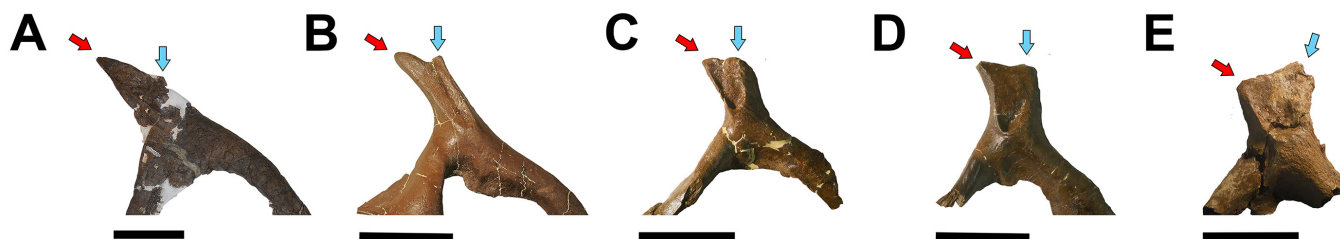


Figure 7. Stratigraphic trends in the nasal process of the premaxilla (NPP). A) TMP 2002.057.0007, the holotype of *Eotriceratops*, from the upper Horseshoe Canyon Formation of Alberta, which slightly predates the HCF (Wu et al. 2007; image mirrored). The NPP is narrow, strongly caudally inclined and exhibits two peaks (red and blue arrows). B) MOR 1122 7-22-00-1, from the base of the HCF. As in *Eotriceratops*, the NPP is forked; however, the peaks are more closely positioned. C) MOR 1120, *Triceratops horridus* from the upper part of the lower unit of the HCF (mirrored). D) MOR 3027, *Triceratops* sp. from the middle unit of the HCF (mirrored). E) MOR 2702, *Triceratops prorsus* from the upper unit of the HCF (mirrored). A, C–E modified from Scannella et al. (2014). Scale, 10 cm.

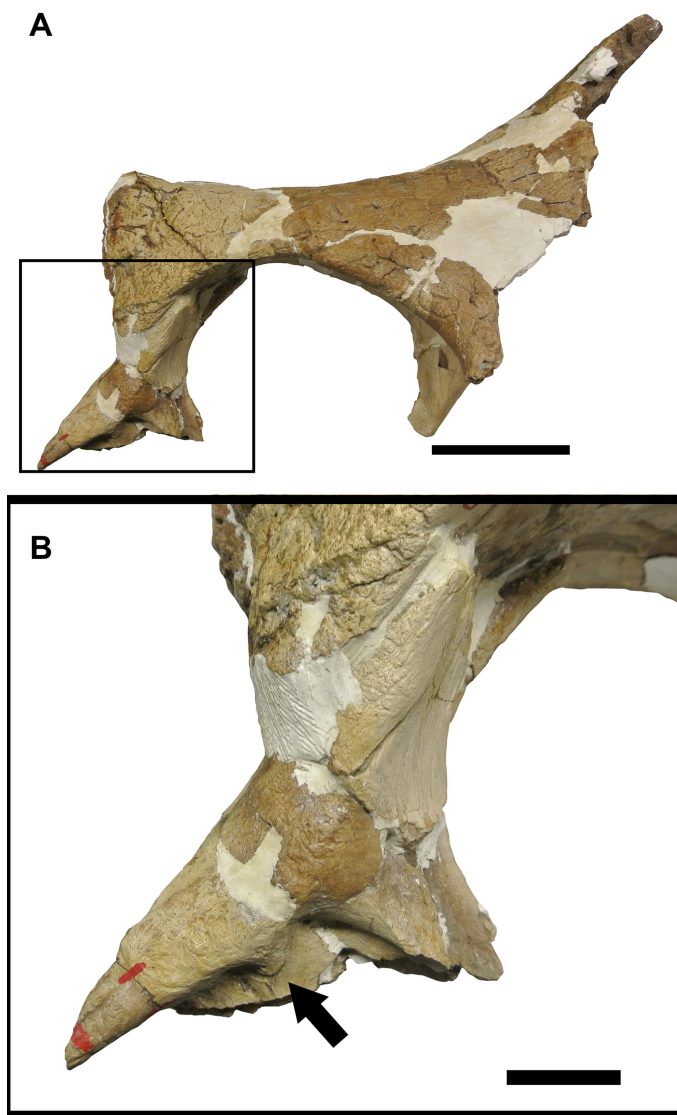


Figure 8. Nasal-premaxilla complex of YPM 1820, the holotype of *Triceratops horridus*. A) Box highlights partial premaxilla. Scale, 10 cm. B) Arrow indicates a strut directed into the interpremaxillary fenestra and positioned well rostral to the narial strut. Scale, 2 cm. Courtesy of the Division of Vertebrate Paleontology; YPM 1820, Peabody Museum of Natural History, Yale University, New Haven, Connecticut, USA; Peabody.yale.edu.

18 cm. The margin where the premaxilla articulates with the rostral bone is relatively thin (approximately 0.5 – 2.2 cm). A foramen is present at the rostroventral corner of the bone, caudal to the rostroventral sulcus. The ventromedial margin of the bone thickens (to approximately 4.5 cm) and becomes slightly convex ventral to the ventromedial chamber and then tapers medially ventral to the premaxillary recess. Several foramina are present on the ventrolateral surface at this point of tapering. A facet for articulation with the maxilla is present at the caudoventral-most preserved point of the bone and exhibits subtle ridges.

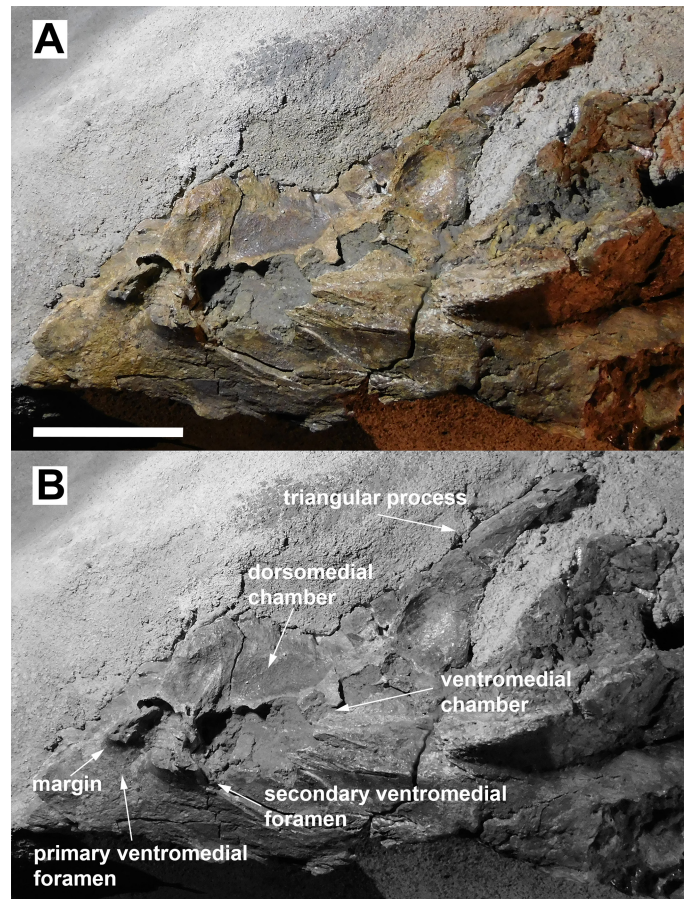


Figure 9. Medial view of the partial right premaxilla of MOR 1122. A) The premaxilla preserves partial ventromedial foramina and portions of the internal chambers. B) The primary ventromedial foramen is partially bound rostrally by an obliquely oriented margin. Though this margin is incomplete, it indicates a minimum diameter of 2.4 cm for the primary foramen. Scale, 10 cm.

PHYLOGENETIC ANALYSIS

In order to assess the systematic position of MOR 1122 7-22-00-1, it was added to the specimen level cladistic analysis of HCF ceratopsid specimens conducted in Scannella et al. 2014. Initially, a branch-and-bound search was performed with MOR 1122 7-22-00-1 added to the Scannella et al. 2014 specimen set which excludes individuals that cannot be coded for at least 10 characters or characters of the frill. The analysis resulted in 49,252 most parsimonious trees with a length of 53 steps, a Consistency Index of 0.74 and a Retention Index of 0.82 (Fig. 12A). *Eotriceratops* was recovered as the most basal member of the ingroup, but in an unresolved position relative to *Arrhinoceratops*. The strict consensus recovers MOR 1122 7-22-00-1 in a polytomy with specimens exhibiting the expanded ‘*Torosaurus*’ frill morphology (MOR 981, MOR 1122, MOR 3081). These specimens exhibit a caudally oriented NPP combined with closely spaced ventromedial foramina (the position of

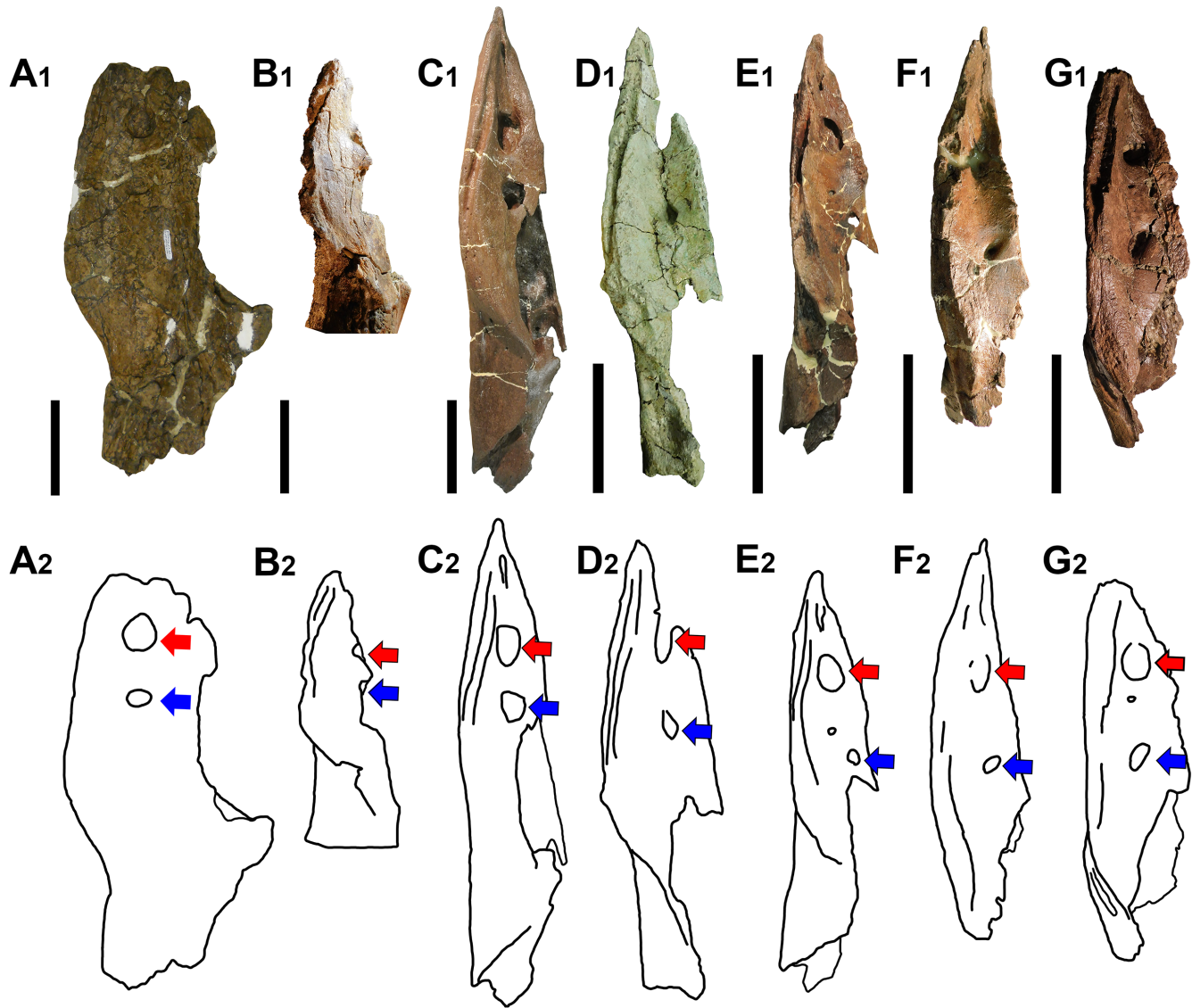


Figure 10. Variation in the ventromedial foramina of the premaxilla (ventral view). A) *Eotriceratops* (TMP 2002.057.0007) exhibits closely spaced primary (red arrow) and secondary (blue arrow) foramina. B) Partially preserved ventromedial foramina of MOR 1122 skull are closely spaced. C) MOR 1122 7-22-00-1 from the basal sandstone of the HCF. D) MOR 3081, a ‘*Torosaurus*’ specimen from upper L3. Though partially crushed, this specimen expresses large, closely spaced ventromedial foramina. E) MOR 1120, *Triceratops horridus* from upper L3 (mirrored). Ventromedial foramina of this specimen are more widely spaced; the distance between the foramina is greater than 1.5 times the width of the primary foramen (character 19; Scannella et al. 2014) F) MOR 3045, *Triceratops* sp. from M3. G) MOR 2971, *Triceratops prorsus* from U3. Scale, 10 cm.

these foramina in MOR 981 was initially coded as ‘?’ (see below). This polytomy is recovered as basal to a stratigraphic succession of other specimens including a large polytomy of specimens from upper M3 and U3. MOR 1122 and MOR 3081 were collected from L3, but the exact stratigraphic position of MOR 981 is unknown (Scannella et al. 2014). MOR 1120, a subadult specimen collected from the upper part of L3, exhibits a caudally oriented NPP and ventromedial foramina which are relatively more widely spaced than those preserved in specimens lower in the formation (Scannella et al. 2014). Specimens recovered from

the upper half of the formation express a more vertically oriented NPP (character 3).

A branch-and-bound search performed using the reduced specimen set (following removal of MOR 2924 from the matrix [Scannella et al. 2014, fig. 3C]) resulted in 1,974 most parsimonious trees with a length of 52 steps, a Consistency Index of 0.75 and a Retention Index of 0.82 (Fig. 12B). The strict consensus tree distinguished upper M3 specimens (MOR 3027, UCMP 113697, MOR 3045) from U3 specimens (Fig. 9B). MOR 3045 and U3 specimens exhibit an expanded NPP (character 13).

Table 2. Measurements of ventromedial foramina (VF) for specimens in Figure 10. Diameter (measured rostrocaudally) and distance between the closest points of the primary and secondary VF. Data presented graphically in Figure 11. Measurements in cm.

Premaxilla	Primary VF Diameter	Secondary VF Diameter	Distance Between VF
TMP 2002.057.0007 [L]	3.8	2*	3.7
TMP 2002.057.0007 [R]	4.4	1.6	5.5
MOR 1122 7-22-00-1	4	2.8	2.9
MOR 1122	2.4**	—	3.4
MOR 3081	3.6	2.1	3.7
MOR 1120 [L]	3.3	1.6	5.5
MOR 1120 [R]	2.5	—	7.4
MOR 3045	2	0.7	5.9
MOR 2971 [L]	2.7	1.8	5.5
MOR 2971 [R]	2.5	1.7	6.2

*The left premaxilla of TMP 2002.057.0007 exhibits a third small VF (1.7 cm diameter) just caudal to the secondary VF.

**MOR 1122 skull VF (Fig. 9) are not fully preserved.

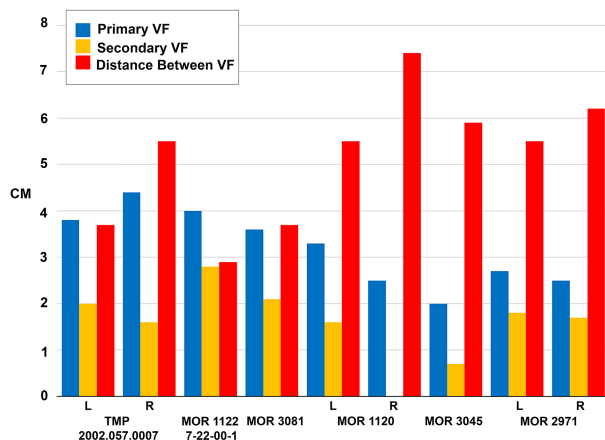


Figure 11. Graphical representation of ventromedial foramina measurement data presented in Table 2. VF, ventromedial foramina. Composed using Microsoft Excel.

Large primary foramina are preserved in MOR 981; however, the relationships of these foramina to surrounding features are somewhat obscured by crushing (see Fig. 13). As such, the character describing the positioning of these foramina (character 19; Scannella et al. 2014) was initially coded as ‘?’ following Scannella et al. 2014. Farke (2007, p. 240) noted the presence of foramina positioned “just rostral to the maxillae” in MOR 981. A version of the analysis using the reduced data set was run with the ventromedial foramina of this specimen coded as being positioned far apart. This analysis resulted in 3,384 most parsimonious trees with a length of 53 steps, a Consistency Index of 0.74 and a Retention Index of 0.81. The strict consensus tree

recovers MOR 981 and all HCF specimens from the lower half of the formation (including MOR 1122 7-22-00-1) in a polytomy (Fig. 12C).

An analysis of the reduced dataset using only premaxilla characters was run after removal of specimens which did not exhibit at least three characters. This analysis resulted in 528 most parsimonious trees with a length of 11 steps, a Consistency Index of 0.91 and a Retention Index of 0.93. The strict consensus tree recovers MOR 1122 7-22-00-1 and MOR 1122 as basal to MOR 1120 and MOR 2982 (from upper L3 and lower M3, respectively) and a polytomy of specimens from the upper half of the formation (Fig. 12D). MOR 1122 7-22-00-1 and MOR 1122 share a deep recess of the triangular process but do not exhibit a prominence just rostral to or descending from the narial strut that is observed in some specimens recovered from higher in the formation (Scannella et al. 2014). Specimens from the upper half of the formation are united by the expression of a more vertically oriented NPP (character 3).

DISCUSSION

The fact that MOR 1122 7-22-00-1 is unfused to surrounding cranial bones might suggest ontogenetic immaturity despite its large size, (see Farke 2011; Longrich and Field 2012); however, cranial fusion alone is an ambiguous indicator of maturity in dinosaurs (Bailleul et al. 2016). The holotype of *Eotriceratops* (TMP 2002.057.0007) is similarly a very large animal with unfused premaxillae (Wu et al. 2007). TMP 2002.057.0007 expresses flattened frill epioffifications and rostrally curved horn cores which are markers of relative maturity in *Triceratopsini* (Horner and Goodwin 2006).

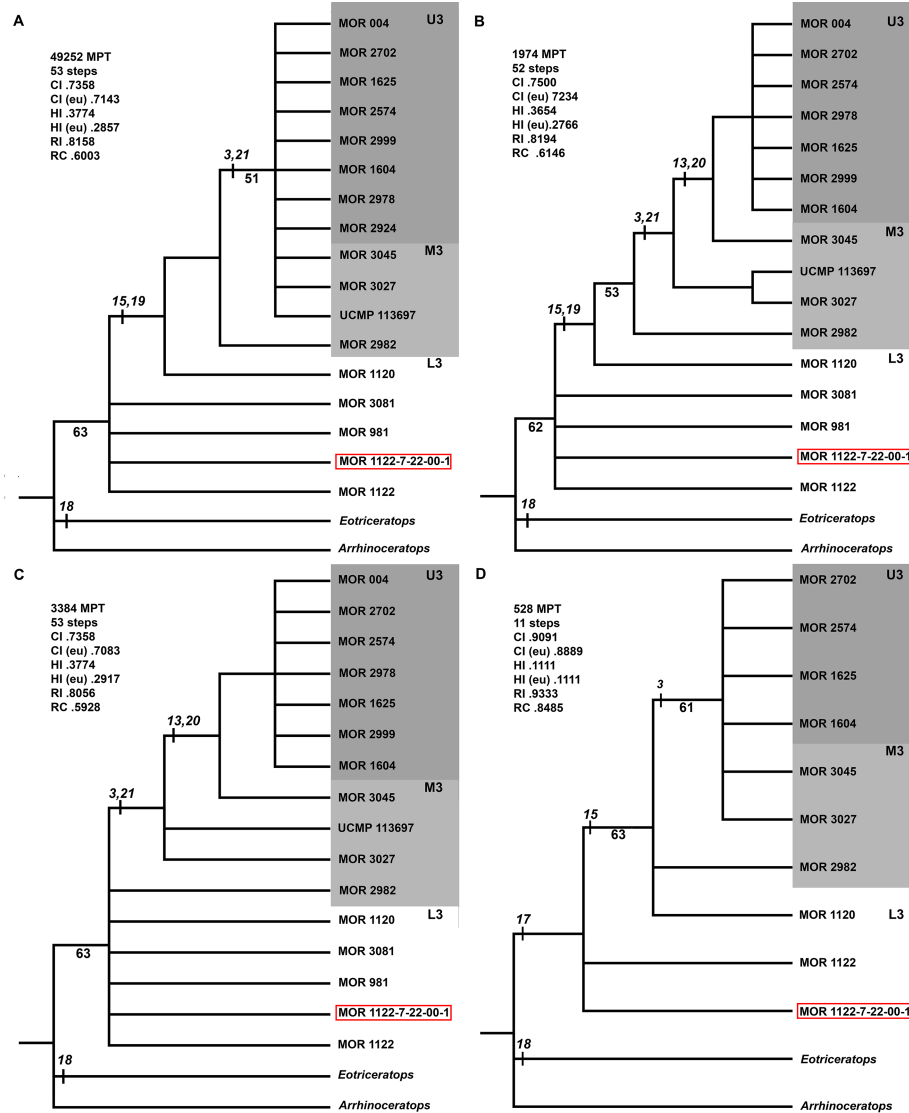


Figure 12. Results of cladistic analyses incorporating MOR 1122 7-22-00-1 into the dataset of Scannella et al. (2014). A) Strict consensus tree excluding specimens from Scannella et al. 2014 that cannot be coded for at least 10 characters or characters of the frill. MOR 1122 7-22-00-1 groups with specimens exhibiting the ‘*Torosaurus*’ morphology. B) Strict consensus tree after removal of MOR 2924. When the positioning of the ventromedial foramina in MOR 981 is coded as ‘?’ MOR 1122 7-22-00-1 groups with specimens exhibiting the ‘*Torosaurus*’ morphology. C) When coding of the ventromedial foramina of MOR 981 is changed to indicate that they are not closely positioned, as suggested by Farke (2007), specimens from L3 are recovered in a polytomy in the strict consensus tree. D) Strict consensus tree when only characters of the premaxilla are included in the analysis and specimens which cannot be coded for at least three characters are removed. Bootstrap support values are presented below nodes. Unambiguously optimized synapomorphies ($0 \rightarrow 1$) present at strict consensus tree internodes are above nodes (numbers correspond to characters in Appendix 1). Stratigraphic positions of MOR 981, MOR 1604, and MOR 2978 are undetermined (Scannella et al. 2014). Abbreviations: MPT, most parsimonious trees; CI, consistency index; HI, homoplasy index; RI, retention index; RC, rescaled consistency index; eu, excluding uninformative characters.

Cladistic analyses recover MOR 1122 7-22-00-1 with HCF specimens exhibiting the expanded ‘*Torosaurus*’ frill morphology (Fig. 12). MOR 1122 7-22-00-1 was found associated with MOR 1122, in which the premaxillae are not well preserved (Farke 2007); however, that skull expresses a narrow, caudally inclined strut extending from the triangular process and closely spaced ventromedial

foramina, consistent with the morphology of MOR 1122 7-22-00-1 (Fig. 10). The incomplete, obliquely oriented rostral margin of the primary ventromedial foramen is positioned rostradorsal to the secondary foramen and extends from within a subtle fossa on the medial surface of the premaxilla (Fig. 9). This may suggest that this margin does not indicate the full extent of the foramen but instead

represents a subdivision of a larger primary foramen. Similarly, a smaller foramen is noted within the primary ventromedial foramen of MOR 1122 7-22-00-1. Closely spaced ventromedial foramina are also observed in MOR 3081, a specimen that exhibits the expanded ‘*Torosaurus*’ frill morphology and was collected from the mudstones of the upper part of L3 (Scannella et al. 2014). MOR 981, another large ‘*Torosaurus*’ skull, expresses a very large (7 cm long) primary foramen on each premaxilla. The relationship of these foramina to surrounding features is partly obscured by crushing (Fig. 13). Farke (2007) noted the presence of foramina just rostral to the maxilla in MOR 981; if these are the secondary foramina, they are positioned well caudal to the primary foramina (approximately 13 cm behind the primary foramina as opposed to 2.9 cm in MOR 1122 7-22-00-1 and a maximum of 7.4 cm in MOR 1120 [Table 2]). Alternatively, it is conceivable that the enlarged primary foramina of MOR 981 may represent the coalescing of adjacent ventromedial foramina. It is worth noting that closely spaced ventromedial foramina have thus far only been reported in HCF specimens with an expanded, fenestrated frill (MOR 1122, MOR 3081; Scannella et al. 2014). These closely spaced foramina may represent a late stage ontogenetic state or be expressed through much or all of ontogeny in individuals from the lowest HCF. The migration of foramina through ontogeny has been noted in several vertebrate groups, (e.g., Watson 1963; Williams and Krovitz 2004) including dinosaurs (Ullmann and Lacovara 2016). If *Triceratops* and ‘*Torosaurus*’ are distinct but closely related taxa, the morphology of these foramina might suggest MOR 1122 7-22-00-1 holds affinities with the latter. However, MOR 981 demonstrates that the size and position of these foramina may not be consistent in all ‘*Torosaurus*’ specimens. Further, the placement of the ventromedial foramina can vary between the right and left sides of unfenestrated specimens (e.g., YPM 1821 figured in Hatcher et al. 1907, fig. 28). Similarly, the right premaxilla of TMP 2002.057.0007 (*Eotriceratops*) exhibits two closely spaced ventromedial foramina whereas the left premaxilla expresses three. Despite this variation, relatively large, closely spaced ventromedial foramina appear to be more commonly recovered low in the HCF (Fig. 10; Scannella et al. 2014).

The morphology of MOR 1122 7-22-00-1 is consistent with its stratigraphic position in the basal sandstone of the HCF. *Eotriceratops*, recovered from Unit 5 of the Horseshoe Canyon Formation (~68.8 Ma; Wu et al. 2007; Eberth and Kamo 2020), has a comparatively simple premaxilla. *Eotriceratops* is diagnosed by its tall, unrecessed triangular process of the premaxilla; a feature which distinguishes it from all HCF specimens recorded to date. The premaxilla of *Eotriceratops* further does not



Figure 13. Ventral view of the premaxillae of MOR 981. White arrows indicate the enlarged primary foramina. Yellow arrow indicates the possible position of the secondary foramen, well caudal to the primary foramina (Farke 2007). Scale, 10 cm.

exhibit a septal flange and the base of the narial strut is not expanded (Fig. 5). In contrast, MOR 1122 7-22-00-1 has a deeply recessed triangular process, a narial strut with an expanded base, and a septal flange positioned along the base of the strut. The recessed triangular process and expanded narial strut morphologies are consistent with other HCF specimens. The presence of a septal flange appears to become less common in HCF ceratopsids, though it is expressed in early ontogeny.

MOR 1122 7-22-00-1 is distinguishable from *Triceratops prorsus*, which is found in the upper unit of the HCF and expresses a much wider and more upright NPP (Forster 1996; Longrich and Field 2012; Scannella et al. 2014). It compares favorably with specimens of *Triceratops horridus* from the lower half of the HCF, in which the NPP is narrow and caudally inclined. The NPP is not everted caudally to the extent observed in *Eotriceratops* and other earlier occurring chasmosaurines where this process is aligned with the rostral ramus of the premaxilla. The forked surface of the NPP of MOR 1122 7-22-00-1 appears to be intermediate between the morphology of *Eotriceratops* and specimens found stratigraphically higher in the HCF (Fig. 7); however, direct comparisons to other specimens from the lower half of the HCF are complicated by the fact that the morphology of this process in similarly large individuals is unknown due to non-preservation (e.g., MOR 1186), taphonomic damage (e.g., MOR 6653; Scannella et al. 2014), or obfuscation due to fusion with adjacent elements (e.g., MOR 981, MOR 1122). Similarly, details of the morphology of the NPP in the holotype of *Triceratops horridus* (YPM 1820) are partially obscured due to articulation with the nasals (Fig. 8) and the specimen does not preserve the ventromedial foramina of the premaxillae. These factors highlight the significance of MOR 1122 7-22-00-1 as a well preserved specimen from a critical stratigraphic zone. In MOR 1122 7-22-00-1, the dorsal surface of the triangular process is elevated above the ventral

margin of the interpremaxillary fenestra, but not quite to the degree observed in *Eotriceratops*. The result is a deeper ventral portion of the premaxilla compared to specimens from higher in the formation (Fig. 5). It is possible that MOR 1122 7-22-00-1 represents a transitional morphology between the stratigraphically lower *Eotriceratops* and specimens found higher in the HCF. Unfortunately, as this individual is represented by a single bone, details of the morphology of the rest of the animal and how they might compare to the associated MOR 1122 skull and other HCF specimens are unknown. It is here referred to *Triceratops* sp.; the discovery of additional well-preserved specimens from the lower HCF will further resolve the range of variation within premaxillae from these strata and allow for direct comparisons with large, unfused specimens (Scannella and Fowler 2014; Fowler 2017).

The elaborate morphology of the premaxilla is one of the features that distinguishes chasmosaurine ceratopsids from centrosaurines, in which the premaxilla is a comparatively simple bone (Dodson et al. 2004). MOR 1122 7-22-00-1 highlights an apparent increase in complexity of the narial region relative to earlier occurring chasmosaurines. Witmer (2001) hypothesized that a rostroventral placement of the nostril in *Triceratops* would provide airflow over the full narial apparatus, facilitating physiological functions. The increased complexity of the chasmosaurine narial region at the onset of HCF deposition may indicate increased physiological or other capabilities in the latest occurring triceratopsins. Further exploration of the basal sandstone of the HCF will continue to clarify ontogenetic sequences throughout the formation, illuminate heterochronic trends, and test evolutionary hypotheses.

ACKNOWLEDGEMENTS

Thank you to the Busenbark and Weaver families for allowing specimens from HC-258 to be collected by MOR. Thanks to K. Olson, R. Harmon, N. Peterson, J. Horner and the MOR field crews which excavated this specimen and Montana Army National Guard, which extracted the HC-258 material. J. Horner and K. Olson provided helpful information about the excavation of the specimen and contextual locality information. I am thankful to C. Brown, T. Carr, A. Farke, D. Fowler, M. Goodwin, M. Holland, J. Horner, M. Loewen, and L. Witmer for helpful conversations, without implying their agreement with conclusions presented here. B. Strilisky and G. Housego (TMP) provided access to TMP 2002.057.0007 at TMP and additional images of the specimen's premaxillae. D. Brinkman, M. Fox, J. Gauthier, and C. Norris provided access to specimens at YPM. Thank you to MOR, MSU, MOR Inc., and the donors to the Hell Creek Project. Thank you to C. Ansell, I. Brenes, S. Brewer, P. Hookey, J. Jette, L. Meld, A. Nash, P. Platt, B. Phillips, L.

Roberts, K. Scannella, and S. Williams for specimen preparation. MOR 1122 reconstruction in Figure 2 completed by M. Holland. Thanks to C. Mehling at AMNH for helping confirm the identification of AMNH FARB 5039. Suggestions by the editor, R. Holmes, and reviewers C. Brown and A. Farke were extremely helpful. C. Brown provided photographs of the holotype of *Regaliceratops* (TMP 2005.055.0001) as well as measurements and additional photographs of the ventromedial foramina of TMP 2002.057.0007 which revealed the presence of three foramina on the left premaxilla. A. Farke shared notes regarding MOR 981. The Bureau of Land Management, United States Fish and Wildlife Service (Charles M. Russell Wildlife Refuge), Montana Department of Natural Resources and Conservation, Montana Fish, Wildlife and Parks, and United States Army Corps of Engineers have permitted MOR access to lands where many HCF ceratopsids have been discovered and continue to contribute to a growing understanding of this group. Special thanks to Kari Scannella, who assisted with photographing TMP 2002.057.0007 and created the graphite illustrations of MOR 1122 7-22-00-1 used in Figure 3.

LITERATURE CITED

- Bailleul, A.M., J.B. Scannella, J.R. Horner, and D.C. Evans. 2016. Fusion patterns in the skulls of modern archosaurs reveal that sutures are ambiguous maturity indicators for the Dinosauria. *PLoS One*, 11(2): e0147687. DOI 10.1371/journal.pone.0147687
- Brown, B. 1907. The Hell Creek beds of the Upper Cretaceous of Montana. *American Museum of Natural History Bulletin* 23:823–845.
- Brown, B. 1917. A complete skeleton of the horned dinosaur *Monoclonius*, and description of a second skeleton showing skin impressions. *Bulletin of the American Museum of Natural History* 37:281–306.
- Brown, C.M., A.P. Russell, and M.J. Ryan. 2009. Pattern and transition of surficial bone texture of the centrosaurine frill and their ontogenetic and taxonomic implications. *Journal of Vertebrate Paleontology* 29:132–141.
- Brown, C.M. and D.M. Henderson. 2015. A new horned dinosaur reveals convergent evolution in cranial ornamentation in Ceratopsidae. *Current Biology* 25:1641–1648.
- Clemens W.A. and J.H. Hartman. 2014. From *Tyrannosaurus rex* to asteroid impact: Early studies (1901–1980) of the Hell Creek Formation in its type area, through the end of the Cretaceous in the type locality of the Hell Creek Formation in Montana and adjacent areas; pp. 1–87 in G.P. Wilson, W.A. Clemens, J.R. Horner, and J.H. Hartman, (eds.), *Geological Society of America Special Paper*, Boulder, Colorado (Special Paper 503).
- Colbert, E.H. and J.D. Bump. 1947. A skull of *Torosaurus* from South Dakota and a revision of the genus. *Proceedings of the Academy of Natural Sciences of Philadelphia* 99:93–106.

- Dodson, P., C.A. Forster, and S.D. Sampson. 2004. Ceratopsidae; pp. 494–513 in Weishampel, D.B., Dodson, P., and H. Osmólska, (eds.), *The Dinosauria*. University of California Press, Berkeley, CA. Second Edition.
- Eberth, D.A. and S.L. Kamo. 2020. High-precision U–Pb CA–ID–TIMS dating and chronostratigraphy of the dinosaur-rich Horseshoe Canyon Formation (Upper Cretaceous, Campanian–Maastrichtian), Red Deer River valley, Alberta, Canada. *Canadian Journal of Earth Sciences*, 57:1220–1237.
- Farke, A.A. 2007. Cranial osteology and phylogenetic relationships of the chasmosaurine ceratopsid *Torosaurus latus*; pp. 235–257 in K. Carpenter (ed.), *Horns and Beaks: Ceratopsian and Ornithomimid Dinosaurs*. Indiana University Press, Bloomington and Indianapolis, Indiana.
- Farke, A.A. 2011. Anatomy and taxonomic status of the chasmosaurine ceratopsid *Nedoceratops hatcheri* from the Upper Cretaceous Lance Formation of Wyoming, USA. *PLoS One*, 6(1).
- Farke, A.A., M.J. Ryan, P.M. Barrett, D.H. Tanke, D.R. Braman, M.A. Loewen, and M.R. Graham. 2011. A new centrosaurine from the Late Cretaceous of Alberta, Canada, and the evolution of parietal ornamentation in horned dinosaurs. *Acta Palaeontologica Polonica* 56:691–702.
- Flight, J.N. 2004. Sequence stratigraphic analysis of the Fox Hills and Hell Creek formations (Maastrichtian). Eastern Montana and its relationship to dinosaur paleontology. MSc thesis, Montana State University, Bozeman, Montana, USA, 149 pp.
- Forster, C.A. 1990. The cranial morphology and systematics of *Triceratops* with a preliminary analysis of ceratopsid phylogeny. Doctoral dissertation, University of Pennsylvania, Philadelphia, PA, USA, 227 pp.
- Forster, C.A. 1996. Species resolution in *Triceratops*: cladistic and morphometric approaches. *Journal of Vertebrate Paleontology* 16:259–270.
- Forster, C.A., P.C. Sereno, T.W. Evans, and T. Rowe. 1993. A complete skull of *Chasmosaurus mariscalensis* (Dinosauria: Ceratopsidae) from the Aguja Formation (late Campanian) of West Texas. *Journal of Vertebrate Paleontology* 13(2):161–170.
- Fowler, D.W. 2009. A sequence stratigraphic subdivision of the Hell Creek Formation: beginnings of a high-resolution regional chronostratigraphic framework for the terminal Cretaceous. 9th North American Paleontological Convention Abstracts. Cincinnati Museum Center Scientific Contributions 3:136.
- Fowler, D.W. 2016. Dinosaurs and time: chronostratigraphic frameworks and their utility in analysis of dinosaur paleobiology. Doctoral dissertation, Montana State University–Bozeman, College of Letters & Science, Bozeman, Montana, USA, 808 pp.
- Fowler, D.W. 2017. Revised geochronology, correlation, and dinosaur stratigraphic ranges of the Santonian–Maastrichtian (Late Cretaceous) formations of the Western Interior of North America. *PLoS ONE* 12(11): e0188426. DOI 10.1371/journal.pone.0188426
- Gates, T.A. and S.D. Sampson. 2007. A new species of *Gryposaurus* (Dinosauria: Hadrosauridae) from the Late Campanian Kaiparowits Formation, southern Utah, USA. *Zoological Journal of the Linnean Society* 151:351–376.
- Goodwin, M.B., W.A. Clemens, J.R. Horner, and K. Padian. 2006. The smallest known *Triceratops* skull: new observations on ceratopsid cranial anatomy and ontogeny. *Journal of Vertebrate Paleontology* 26:103–112.
- Hartman, J.H., R.D. Butler, M.W. Weiler, and K.K. Schumaker. 2014. Context, naming, and formal designation of the Cretaceous Hell Creek Formation lectostratotype, Garfield County, Montana; pp. 313–332 in G.P. Wilson, W.A. Clemens, J.R. Horner, and J.H. Hartman (eds.), *Through the End of the Cretaceous in the Type Locality of the Hell Creek Formation in Montana and Adjacent Areas*. Geological Society of America Special Paper 503, Boulder, Colorado.
- Hatcher, J.B., O.C. Marsh, and R.S. Lull. 1907. *The Ceratopsia*. US Geological Survey Monograph 49:1–300.
- Holmes, R.B., C.A. Forster, M.J. Ryan, and K.M. Shepherd. 2001. A new species of *Chasmosaurus* (Dinosauria: Ceratopsia) from the Dinosaur Park Formation of Southern Alberta. *Canadian Journal of Earth Sciences* 38:1423–1438.
- Horner, J.R. and M.B. Goodwin. 2006. Major cranial changes during *Triceratops* ontogeny. *Proceedings of the Royal Society B* 273:2757–2761.
- Horner, J.R. and M.B. Goodwin. 2008. Ontogeny of cranial epi-ossifications in *Triceratops*. *Journal of Vertebrate Paleontology* 28:134–144.
- Horner, J.R. and E.T. Lamm. 2011. Ontogeny of the parietal frill of *Triceratops*: a preliminary histological analysis. *Comptes Rendus Palevol* 10:439–452.
- Horner, J.R., M.B. Goodwin, and N. Myhrvold. 2011. Dinosaur census reveals abundant *Tyrannosaurus* and rare ontogenetic stages in the Upper Cretaceous Hell Creek Formation (Maastrichtian), Montana, USA. *PLoS ONE* 6(2): e16574. DOI 10.1371/journal.pone.0016574
- Loewen, M.A., S.D. Sampson, E.K. Lund, A.A. Farke, M.C. Aguillón-Martínez, C.A. de Leon, R.A. Rodríguez-de la Rosa, M.A. Getty, and D.A. Eberth. 2010. Horned dinosaurs (Ornithischia: Ceratopsidae) from the Upper Cretaceous (Campanian) Cerro del Pueblo Formation, Coahuila, Mexico; pp. 99–116 in M.J. Ryan, B. Chinnery-Allgeier, and D.A. Eberth (eds.), *New Perspectives on Horned Dinosaurs: The Royal Tyrrell Museum Ceratopsian Symposium*. Indiana University Press, Bloomington, Indiana, USA.
- Longrich, N.R. 2010. *Mojoceratops perifania*, a new chasmosaurine ceratopsid from the Late Campanian of Western Canada. *Journal of Paleontology* 84(4):681–694.
- Longrich, N.R. 2011. *Titanoceratops ouranos*, a giant horned dinosaur from the late Campanian of New Mexico. *Cretaceous Research* 32:264–276.

- Longrich, N.R. and D.J. Field. 2012. *Torosaurus* is not *Triceratops*: ontogeny in chasmosaurine ceratopsids as a case study in dinosaur taxonomy. *PLoS One* 7(2).
- Mallon, J.C., C.J. Ott, P.L. Larson, E.M. Iuliano, and D.C. Evans. 2016. *Spichypeus shipporum* gen. et sp. nov., a boldly audacious new chasmosaurine ceratopsid (Dinosauria: Ornithischia) from the Judith River Formation (Upper Cretaceous: Campanian) of Montana, USA. *PLoS One* 11(5).
- Marsh, O.C. 1891. Notice of new vertebrate fossils. *American Journal of Science*, series 3:265–269.
- Maiorino, L., A.A. Farke, T. Kotsakis, and P. Piras. 2013. Is *Torosaurus Triceratops*? Geometric morphometric evidence of late Maastrichtian ceratopsid dinosaurs. *PLoS ONE* 8(11): e81608. DOI 10.1371/journal.pone.0081608
- McDonald, A.T., C.E. Campbell, and B. Thomas. 2016. A new specimen of the controversial chasmosaurine *Torosaurus latus* (Dinosauria: Ceratopsidae) from the Upper Cretaceous Hell Creek Formation of Montana. *PLoS ONE* 11(3): e0151453. DOI 10.1371/journal.pone.0151453
- McDonald, A.T., D.G. Wolfe, and J.I. Kirkland. 2010. A new basal hadrosauroid (Dinosauria: Ornithopoda) from the Turonian of New Mexico. *Journal of Vertebrate Paleontology* 3:799–812.
- Ostrom, J.H. and P. Wellnhofer. 1986. The Munich specimen of *Triceratops* with a revision of the genus. *Zitteliana* 14:111–158.
- Rambaut A. 2012. FigTree. Version 1.4.0. Available at <http://tree.bio.ed.ac.uk/software/figtree/>.
- Sampson, S. D., M.A. Loewen, A.A. Farke, E.M. Roberts, C.A. Forster, J.A. Smith, and A.L. Titus. 2010. New horned dinosaurs from Utah provide evidence for intracontinental dinosaur endemism. *PLOS ONE* 5(9): e12292. DOI 10.1371/journal.pone.0012292
- Scannella, J.B. and J.R. Horner. 2010. *Torosaurus* Marsh, 1891, is *Triceratops* Marsh, 1889 (Ceratopsidae: Chasmosaurinae): synonymy through ontogeny. *Journal of Vertebrate Paleontology* 30:1157–1168.
- Scannella, J.B. and J.R. Horner. 2011. '*Nedoceratops*': an example of a transitional morphology. *PLoS ONE* 6(12): e28705. DOI 10.1371/journal.pone.0028705
- Scannella, J. B. and D.W. Fowler. 2014. A stratigraphic survey of *Triceratops* localities in the Hell Creek Formation, northeastern Montana (2006–2010); pp. 313–332 in G.P. Wilson, W.A. Clemens, J.R. Horner, and J.H. Hartman (eds.), *Through the End of the Cretaceous in the Type Locality of the Hell Creek Formation in Montana and Adjacent Areas*. Geological Society of America Special Paper 503, Boulder, Colorado.
- Scannella, J.B., D.W. Fowler, M.B. Goodwin, and J.R. Horner. 2014. Evolutionary trends in *Triceratops* from the Hell Creek Formation, Montana. *Proceedings of the National Academy of Sciences of the United States* 111:10245–10250.
- Schweitzer, M. H., J.L. Wittmeyer, J.R. Horner, and J.K. Toporski. 2005. Soft-tissue vessels and cellular preservation in *Tyrannosaurus rex*. *Science* 307(5717):1952–1955.
- Sullivan, R.M., A.C. Boere, and S.G. Lucas. 2005. Redescription of the ceratopsid dinosaur *Torosaurus utahensis* (Gilmore, 1946) and a revision of the genus. *Journal of Paleontology* 79(3):564–582.
- Swofford D.L. 2002. PAUP*: Phylogenetic Analysis Using Parsimony (*and Other Methods) (Sinauer Associates, Sunderland, MA), Version 4.
- Ullmann, P.V., and K.J. Lacovara. 2016. Appendicular osteology of *Dreadnoughtus schrani*, a giant titanosaurian (Sauropoda, Titanosauria) from the Upper Cretaceous of Patagonia, Argentina. *Journal of Vertebrate Paleontology* 36(6), e1225303.
- Watson, D.M.S. 1963. On growth stages in branchiosaurs. *Palaeontology* 6:540–553.
- Williams, F.L.E., and G.E. Krovitz. 2004. Ontogenetic migration of the mental foramen in Neandertals and modern humans. *Journal of Human Evolution* 47:199–219.
- Wilson, J.P. and D.W. Fowler. 2017. First confirmed identification of juvenile *Triceratops* epiparietals. *Cretaceous Research* 70:71–76.
- Witmer, L. M. 2001. Nostril position in dinosaurs and other vertebrates and its significance for nasal function. *Science* 293(5531):850–853.
- Wu, X.C., D.B. Brinkman, D.A. Eberth, and D.R. Braman. 2007. A new ceratopsid dinosaur (Ornithischia) from the uppermost Horseshoe Canyon Formation (upper Maastrichtian), Alberta, Canada. *Canadian Journal of Earth Sciences* 44:1243–1265.

Appendix 1. Characters used in cladistic analysis (from Scannella et al., 2014).

- 1) Postorbital horn-core length: (0) long (postorbital horn-core/basal-skull length ratio: ≥ 0.64); (1) short (postorbital horn-core/basal-skull length ratio: < 0.64) (Forster 1990: character 58 modified; Forster 1996: character 2 modified).
- 2) Cross-section of postorbital horn core: (0) circular to subcircular; (1) narrow.
- 3) Rostrum shape: (0) primary axis of nasal process of premaxilla (NPP) is strongly posteriorly inclined; (1) NPP vertical or nearly vertical (Forster 1996: character 4 modified; Longrich and Field 2012).
- 4) Frontoparietal fontanelle: (0) open fontanelle; (1) closed or constricted due to fusion of frontals and parietals; (Forster 1990: characters 49 and 50 modified (Forster 1996: character 3 modified).
- 5) Epijugal: (0) comes to a pronounced peak; (1) low and blunt (Longrich 2010: character 102 modified; Sampson et al., 2010: character 50 modified).
- 6) Quadratojugal notch: (0) present; (1) absent (sensu Gates and Sampson 2007: character 71; and McDonald et al. 2010: character 16).
- 7) Nasal-horn length: (0) short (length/width ratio < 1.85); (1) long (length/width ratio > 1.85) (Forster 1990: character 28 modified; Forster 1996: character 5 modified).
- 8) Dorsal surface of epinasal: (0) narrow to peaked; (1) broad.
- 9) Nasal: (0) short, arched; (1) elongate, straight.
- 10) protuberance posterior to epinasal: (0) very subtle or absent; (1) present, prominent; (2) enlarged into a pronounced bump or boss (see Ostrom and Wellnhofer 1986, and Forster 1996).
- 11) Anteromedial process on nasal: (0) present, pronounced; (1) reduced, constricted or absent.
- 12) Posterior projection on epinasal: (0) present; (1) absent.
- 13) Nasal process of the premaxilla: (0) narrow; (1) expanded.
- 14) Midline peak on nasal process of the premaxilla: (0) absent; (1) present.
- 15) Prominence immediately anterior to or descending from the narial strut, directed into interpremaxillary fenestra: (0) absent; (1) present.
- 16) Premaxilla, accessory strut in septal fossa: (0) no accessory strut; (1) strut present (Sampson et al. 2010: character 12).
- 17) Premaxilla, triangular process recess: (0) shallow; (1) deep (Dodson et al. 2004: character 12 modified).
- 18) Triangular (“narial,” sensu Wu et al. 2007) process of premaxilla: (0) dorsal margin (at point of contact with narial strut) positioned roughly at or below the ventral margin of the interpremaxillary fenestra; (1) dorsal margin of narial process (at point of contact with narial strut) positioned well above ventral margin of interpremaxillary fenestra (Wu et al. 2007).
- 19) Ventromedial foramina of the premaxilla positioned (0) close together or (1) far apart (more than 1.5 times the width of anterior foramen).
- 20) Posteroventral surface of the posterior “prong” of premaxilla (sensu Wu et al. 2007): (0) comes to a narrow ridge; (1) broad posterior surface.
- 21) Posterior prong of premaxilla: (0) broad surface for articulation with nasal; (1) exhibits a pronounced ridge on the lateral surface and a constricted area for articulation with the nasal.
- 22) Episquamosal or squamosal crenulation number (Farke et al. 2011: character 55 modified): (0) seven or more; (1) six or fewer.
- 23) Convex margin of squamosal (0) absent; (1) present (Longrich and Field 2012)
- 24) Anterolateral projection on squamosal: (0) present, projects anteriorly producing strongly concave anterior margin of the squamosal; (1) anterior projection present but does not project strongly anteriorly; (2) greatly reduced or absent (Sullivan et al. 2005).
- 25) Squamosal bar (0) present; (1) absent (Forster 1990: character 90 modified; Sampson et al. 2010: character 64 modified).
- 26) Ventral surface of parietal in areas surrounding fenestrae/incipient fenestrae: (0) smooth transition in thickness; (1) thickness transitions in pronounced step from thicker to thinner bone.
- 27) Number of epiparietals or parietal crenulations per side of parietal: (0) four or fewer; (1) five; (2) six or more (Holmes et al. 2001: character 28 modified; Forster 1990: character 46 modified; Sampson et al. 2010: character 93 modified).
- 28) Parietal fenestrae: (0) present; (1) absent (Forster 1990: character 84 modified).
- 29) Epiossification or crenulation on midline of parietal: (0) absent; (1) present (Sampson et al. 2010: character 95 modified; Forster, 1996).
- 30) Epiossification or crenulation spanning parietal-squamosal contact: (0) absent; (1) present (Farke et al. 2011: character 43 modified).

Appendix 2. Character matrix from Scannella et al. 2014 with the addition of MOR 1122 7-22-00-1. MOR 981 was initially coded as “?” for character 19 (position of ventromedial foramina); an additional analysis was run with this coding changed to “1” following Farke, 2007 (see Discussion). Nexus files from Scannella et al. 2014 available at Morphobank.org (project number 1099).

ROM796	00010 ?0001 ????? ?00?? ?0000 (01)000?
TMP 2002.057.0007	0?0?0 000?? ??000 0010? ????? ???0
MOR1122	10010 00101 ???0 ?1?0? ?0000 (01)2001
MOR 1122 7-22-00-1	??0?? ????? ??000 1100? ????? ?????
MOR3081	10??0 ?00?1 ????? ???0? ?0010 01000
MOR1120	1000? 00101 0?001 11?10 0(01)(01)01 00?10
MOR2552	00?01 ????? ????? ????? ???1 ???1
MOR2985	????? ????? ????? ????? ??011 0????
MOR3005	????? ???0? 0???? ????? 0???? 0????1
MOR2982	1?0?1 ?01?2 ??0?1 1???? 0??1? ?????
MOR3010	1???? ?01?1 0???? ????? ????? ?????
MOR3011	??0?? ?01?? 000?0 1???? ????? ?????
UCMP113697	0010? ?11?2 ????? ????? 1?111 ?0110
MOR3027	0?10? 0??1? 00001 01?10 1?011 00?01
MOR3045	1010? 0?1?? 00111 ???11 11011 10110
UCMP128561	????? ?01?? ????? 1???? ????? ?????
MOR2574	101?? ?101? 11101 11??? ???1 0??0?
MOR2702	?11?? 010?0 ??10? 1???1 1?021 1????
MOR1625	??1?0 ?10?0 ????? 1101? ?1121 1????
MOR2924	??1?? ?111? ?11?? ?1??1 11111 1?1??
MOR2978	1??1? ?1010 ????? ????? ??121 1?1??
UCMP136092	1???? ????? ????? ????? ?1111 ?11??
MOR2936	????? 01??? ?11?? 0???1 1??2? ?????
MOR2979	11?1? 0???? ????? ???1 1???? ???0
MOR2971	??1?? ?10?0 ??1?1 1101? ????? ?????
UCMP137263	10??? ???1? 1???? ????? ???1 ?????0
MOR004	??111 ?1010 ????? ????? ?11?1 ?0110
MOR2999	10?0? 1??1? 1???? ????? ?1(01)(12)1 10?10
MOR2923	11?1? ?101? ????? ????? ????? ?010?
MOR1604	1?1?1 01110 ????? 11??? ???2? ?????
MOR981	0?0?? ?010? ????? ????? ????? 01001
